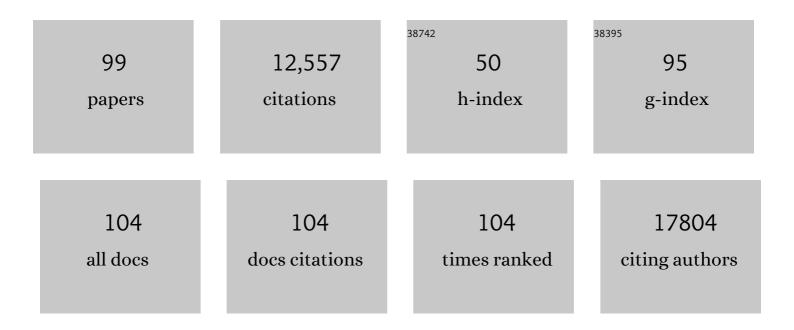


List of Publications by Year in descending order

Source: https://exaly.com/author-pdf/9253036/publications.pdf Version: 2024-02-01



VI VII

#	Article	IF	CITATIONS
1	Niobium Tungsten Oxides for Electrochromic Devices with Long-Term Stability. ACS Nano, 2022, 16, 2621-2628.	14.6	44
2	Kinetics-Controlled Super-Assembly of Asymmetric Porous and Hollow Carbon Nanoparticles as Light-Sensitive Smart Nanovehicles. Journal of the American Chemical Society, 2022, 144, 1634-1646.	13.7	64
3	High-resolution transmission electron microscopy of beam-sensitive halide perovskites. CheM, 2022, 8, 327-339.	11.7	9
4	Atomic Tuning of Single-Atom Fe–N–C Catalysts with Phosphorus for Robust Electrochemical CO ₂ Reduction. Nano Letters, 2022, 22, 1557-1565.	9.1	111
5	Revealing the spatial and temporal distribution of different chemical states of lithium by EELS analysis using non-negative matrix factorization. Micron, 2022, 154, 103213.	2.2	1
6	Circumferential Li metal deposition at high rates enabled by the synergistic effect of a lithiophilic and ionic conductive network. Journal of Materials Chemistry A, 2022, 10, 5391-5401.	10.3	4
7	Engineering Lattice Disorder on a Photocatalyst: Photochromic BiOBr Nanosheets Enhance Activation of Aromatic C–H Bonds via Water Oxidation. Journal of the American Chemical Society, 2022, 144, 3386-3397.	13.7	96
8	Microstructure of Lithium Dendrites Revealed by Room-Temperature Electron Microscopy. Journal of the American Chemical Society, 2022, 144, 4124-4132.	13.7	12
9	Synthesis of a Spatially Confined, Highly Durable, and Fully Exposed Pd Cluster Catalyst via Sequential Site-Selective Atomic Layer Deposition. ACS Applied Materials & Interfaces, 2022, 14, 14466-14473.	8.0	6
10	Self-assembled Pt–CoFe layered double hydroxides for efficient alkaline water/seawater splitting by spontaneous redox synthesis. Journal of Power Sources, 2022, 532, 231353.	7.8	20
11	<i>In Situ</i> Growth of Strained Matrix on CsPbl ₃ Perovskite Quantum Dots for Balanced Conductivity and Stability. ACS Nano, 2022, 16, 10534-10544.	14.6	16
12	Direct aerobic oxidation of monoalcohol and diols to acetals using tandem Ru@MOF catalysts. Nano Research, 2021, 14, 479-485.	10.4	27
13	Ambipolar two-dimensional bismuth nanostructures in junction with bismuth oxychloride. Nano Research, 2021, 14, 1103-1109.	10.4	6
14	All‣olid‣tate Batteries with a Limited Lithium Metal Anode at Room Temperature using a Garnetâ€Based Electrolyte. Advanced Materials, 2021, 33, e2002325.	21.0	99
15	Living materials fabricated via gradient mineralization of light-inducible biofilms. Nature Chemical Biology, 2021, 17, 351-359.	8.0	85
16	Manganese vacancy-confined single-atom Ag in cryptomelane nanorods for efficient Wacker oxidation of styrene derivatives. Chemical Science, 2021, 12, 6099-6106.	7.4	22
17	High-performance overall water splitting based on amorphous iron doped cobalt tungstate <i>via</i> facile co-precipitation. Journal of Materials Chemistry A, 2021, 9, 9753-9760.	10.3	34
18	Pyroelectric nanoplates for reduction of CO2 toÂmethanol driven by temperature-variation. Nature Communications, 2021, 12, 318.	12.8	51

#	Article	IF	CITATIONS
19	The effects of local strain on the cubic Li7La3Zr2O12(001)/Li(001) interface: A first-principles study. Solid State Ionics, 2021, 360, 115546.	2.7	5
20	Layer-by-layer anionic diffusion in two-dimensional halide perovskite vertical heterostructures. Nature Nanotechnology, 2021, 16, 584-591.	31.5	88
21	Improved Electrochemical Performance of Li-Rich Layered Oxide Cathodes Enabled by a Two-Step Heat Treatment. ACS Applied Materials & Interfaces, 2021, 13, 13281-13288.	8.0	15
22	<i>In Situ</i> Probing the Kinetics of Gold Nanoparticle Thermal Sintering in Liquids: Implications for Ink-Jet Printing. ACS Applied Nano Materials, 2021, 4, 2538-2546.	5.0	4
23	Probing the Formation of Lithium Metal in an Inert Atmosphere by Big Data-Driven <i>In Situ</i> Electron Microscopy. ACS Applied Energy Materials, 2021, 4, 7226-7232.	5.1	2
24	Electrocatalytic NiCo ₂ O ₄ Nanofiber Arrays on Carbon Cloth for Flexible and High-Loading Lithium–Sulfur Batteries. Nano Letters, 2021, 21, 5285-5292.	9.1	64
25	Pr-Doped LaCoO ₃ toward Stable and Efficient Oxygen Evolution Reaction. ACS Applied Energy Materials, 2021, 4, 9057-9065.	5.1	15
26	Cation/Anion Codoped and Cobalt-Free Li-Rich Layered Cathode for High-Performance Li-Ion Batteries. Nano Letters, 2021, 21, 8370-8377.	9.1	35
27	Calcium-Assisted <i>In Situ</i> Formation of Perovskite Nanocrystals for Luminescent Green and Blue Emitters. ACS Applied Nano Materials, 2021, 4, 14303-14311.	5.0	3
28	Towards atomic-scale electron microscopy characterization of single molecular catalysts. Catalysis Today, 2020, 350, 192-196.	4.4	2
29	Stabilized lithium metal anode by an efficient coating for high-performance Li–S batteries. Energy Storage Materials, 2020, 24, 329-335.	18.0	79
30	Unravelling the room-temperature atomic structure and growth kinetics of lithium metal. Nature Communications, 2020, 11, 5367.	12.8	29
31	Enhanced Oxygen Evolution Activity of CoO–La _{0.7} Sr _{0.3} MnO _{3â^î^} Heterostructured Thin Film. ACS Applied Energy Materials, 2020, 3, 7988-7996.	5.1	15
32	Rapid defect characterization: The efficiency of diffraction contrastâ€scanning transmission electron microscopy. Microscopy Research and Technique, 2020, 83, 1604-1609.	2.2	0
33	Morphology-controlled transformation of Cu@Au core-shell nanowires into thermally stable Cu3Au intermetallic nanowires. Nano Research, 2020, 13, 2564-2569.	10.4	22
34	Covalent Triazine Framework Confined Copper Catalysts for Selective Electrochemical CO ₂ Reduction: Operando Diagnosis of Active Sites. ACS Catalysis, 2020, 10, 4534-4542.	11.2	112
35	Two-dimensional halide perovskite lateral epitaxial heterostructures. Nature, 2020, 580, 614-620.	27.8	284
36	Highâ€Performance Threeâ€Dimensional Li Anode Scaffold Enabled by Homogeneous Zn Nanoclusters. Small, 2020, 16, e2001257.	10.0	25

#	Article	IF	CITATIONS
37	Engineering plasticization resistant gas separation membranes using metal–organic nanocapsules. Chemical Science, 2020, 11, 4687-4694.	7.4	22
38	Atomic-scale study of nanocatalysts by aberration-corrected electron microscopy. Journal of Physics Condensed Matter, 2020, 32, 413004.	1.8	2
39	Structural Damage of Two-Dimensional Organic–Inorganic Halide Perovskites. Inorganics, 2020, 8, 13.	2.7	5
40	Spontaneous Delithiation under <i>Operando</i> Condition Triggers Formation of an Amorphous Active Layer in Spinel Cobalt Oxides Electrocatalyst toward Oxygen Evolution. ACS Catalysis, 2019, 9, 7389-7397.	11.2	52
41	Highâ€Performance, Lowâ€Cost, and Denseâ€6tructure Electrodes with High Mass Loading for Lithiumâ€lon Batteries. Advanced Functional Materials, 2019, 29, 1903961.	14.9	93
42	Molecular engineering of organic–inorganic hybrid perovskites quantum wells. Nature Chemistry, 2019, 11, 1151-1157.	13.6	302
43	A generalizable method for the construction of MOF@polymer functional composites through surface-initiated atom transfer radical polymerization. Chemical Science, 2019, 10, 1816-1822.	7.4	75
44	MXene (Ti ₃ C ₂) Vacancy-Confined Single-Atom Catalyst for Efficient Functionalization of CO ₂ . Journal of the American Chemical Society, 2019, 141, 4086-4093.	13.7	479
45	Extrinsic and Dynamic Edge States of Two-Dimensional Lead Halide Perovskites. ACS Nano, 2019, 13, 1635-1644.	14.6	79
46	General Way To Construct Micro- and Mesoporous Metal–Organic Framework-Based Porous Liquids. Journal of the American Chemical Society, 2019, 141, 19708-19714.	13.7	111
47	Understanding the formation of multiply twinned structure in decahedral intermetallic nanoparticles. IUCrJ, 2019, 6, 447-453.	2.2	13
48	Strongly Quantum Confined Colloidal Cesium Tin Iodide Perovskite Nanoplates: Lessons for Reducing Defect Density and Improving Stability. Nano Letters, 2018, 18, 2060-2066.	9.1	128
49	Bacteria photosensitized by intracellular gold nanoclusters for solar fuel production. Nature Nanotechnology, 2018, 13, 900-905.	31.5	362
50	Electrical and Optical Tunability in All-Inorganic Halide Perovskite Alloy Nanowires. Nano Letters, 2018, 18, 3538-3542.	9.1	51
51	MOFâ€Confined Subâ€2 nm Atomically Ordered Intermetallic PdZn Nanoparticles as Highâ€Performance Catalysts for Selective Hydrogenation of Acetylene. Advanced Materials, 2018, 30, e1801878.	21.0	133
52	Phase-transition–induced p-n junction in single halide perovskite nanowire. Proceedings of the National Academy of Sciences of the United States of America, 2018, 115, 8889-8894.	7.1	48
53	Benzoin Radicals as Reducing Agent for Synthesizing Ultrathin Copper Nanowires. Journal of the American Chemical Society, 2017, 139, 3027-3032.	13.7	40
54	Structural, optical, and electrical properties of phase-controlled cesium lead iodide nanowires. Nano Research, 2017, 10, 1107-1114.	10.4	128

#	Article	IF	CITATIONS
55	Ultrathin Epitaxial Cu@Au Core–Shell Nanowires for Stable Transparent Conductors. Journal of the American Chemical Society, 2017, 139, 7348-7354.	13.7	125
56	Tandem Catalysis for CO ₂ Hydrogenation to C ₂ –C ₄ Hydrocarbons. Nano Letters, 2017, 17, 3798-3802.	9.1	183
57	Strain-Mediated Coexistence of Volatile and Nonvolatile Converse Magnetoelectric Effects in Fe/Pb(Mg _{1/3} Nb _{2/3}) _{0.7} Ti _{0.3} O ₃ Heterostructure. ACS Applied Materials & Interfaces, 2017, 9, 20637-20647.	8.0	32
58	Electrochemical Activation of CO ₂ through Atomic Ordering Transformations of AuCu Nanoparticles. Journal of the American Chemical Society, 2017, 139, 8329-8336.	13.7	529
59	Room-Temperature Dynamics of Vanishing Copper Nanoparticles Supported on Silica. Nano Letters, 2017, 17, 2732-2737.	9.1	27
60	Atomic structure of sensitive battery materials and interfaces revealed by cryo–electron microscopy. Science, 2017, 358, 506-510.	12.6	1,039
61	Ultralow thermal conductivity in all-inorganic halide perovskites. Proceedings of the National Academy of Sciences of the United States of America, 2017, 114, 8693-8697.	7.1	246
62	Ruddlesden–Popper Phase in Two-Dimensional Inorganic Halide Perovskites: A Plausible Model and the Supporting Observations. Nano Letters, 2017, 17, 5489-5494.	9.1	90
63	Control of Architecture in Rhombic Dodecahedral Pt–Ni Nanoframe Electrocatalysts. Journal of the American Chemical Society, 2017, 139, 11678-11681.	13.7	166
64	Synthesis of Composition Tunable and Highly Luminescent Cesium Lead Halide Nanowires through Anion-Exchange Reactions. Journal of the American Chemical Society, 2016, 138, 7236-7239.	13.7	397
65	Atomic Structure of Ultrathin Gold Nanowires. Nano Letters, 2016, 16, 3078-3084.	9.1	82
66	Growth and Photoelectrochemical Energy Conversion of Wurtzite Indium Phosphide Nanowire Arrays. ACS Nano, 2016, 10, 5525-5535.	14.6	70
67	Ultrathin Colloidal Cesium Lead Halide Perovskite Nanowires. Journal of the American Chemical Society, 2016, 138, 13155-13158.	13.7	234
68	Directed Assembly of Nanoparticle Catalysts on Nanowire Photoelectrodes for Photoelectrochemical CO ₂ Reduction. Nano Letters, 2016, 16, 5675-5680.	9.1	125
69	Insights into the Mechanism of Tandem Alkene Hydroformylation over a Nanostructured Catalyst with Multiple Interfaces. Journal of the American Chemical Society, 2016, 138, 11568-11574.	13.7	82
70	Anisotropic phase segregation and migration of Pt in nanocrystals en route to nanoframe catalysts. Nature Materials, 2016, 15, 1188-1194.	27.5	244
71	Atomic Resolution Imaging of Halide Perovskites. Nano Letters, 2016, 16, 7530-7535.	9.1	125
72	A Molecular Surface Functionalization Approach to Tuning Nanoparticle Electrocatalysts for Carbon Dioxide Reduction. Journal of the American Chemical Society, 2016, 138, 8120-8125.	13.7	340

#	Article	IF	CITATIONS
73	Thermal Transport in Silicon Nanowires at High Temperature up to 700 K. Nano Letters, 2016, 16, 4133-4140.	9.1	74
74	Solution-Processed Copper/Reduced-Graphene-Oxide Core/Shell Nanowire Transparent Conductors. ACS Nano, 2016, 10, 2600-2606.	14.6	155
75	Synthesis of PtCo3 polyhedral nanoparticles and evolution to Pt3Co nanoframes. Surface Science, 2016, 648, 328-332.	1.9	42
76	Low-Temperature Solution-Phase Growth of Silicon and Silicon-Containing Alloy Nanowires. Journal of Physical Chemistry C, 2016, 120, 20525-20529.	3.1	4
77	Core–Shell CdS–Cu ₂ S Nanorod Array Solar Cells. Nano Letters, 2015, 15, 4096-4101.	9.1	114
78	Stabilization of 4H hexagonal phase in gold nanoribbons. Nature Communications, 2015, 6, 7684.	12.8	215
79	Growth and Anion Exchange Conversion of CH ₃ NH ₃ PbX ₃ Nanorod Arrays for Light-Emitting Diodes. Nano Letters, 2015, 15, 5519-5524.	9.1	342
80	Solution-Phase Synthesis of Cesium Lead Halide Perovskite Nanowires. Journal of the American Chemical Society, 2015, 137, 9230-9233.	13.7	861
81	Solution Phase Synthesis of Indium Gallium Phosphide Alloy Nanowires. ACS Nano, 2015, 9, 3951-3960.	14.6	44
82	Genetic and biochemical investigations of the role of MamP in redox control of iron biomineralization in <i>Magnetospirillum magneticum</i> . Proceedings of the National Academy of Sciences of the United States of America, 2015, 112, 3904-3909.	7.1	62
83	Atomically thin two-dimensional organic-inorganic hybrid perovskites. Science, 2015, 349, 1518-1521.	12.6	1,159
84	Synthesis of Ultrathin Copper Nanowires Using Tris(trimethylsilyl)silane for High-Performance and Low-Haze Transparent Conductors. Nano Letters, 2015, 15, 7610-7615.	9.1	179
85	Hybrid bioinorganic approach to solar-to-chemical conversion. Proceedings of the National Academy of Sciences of the United States of America, 2015, 112, 11461-11466.	7.1	234
86	Phase-Selective Cation-Exchange Chemistry in Sulfide Nanowire Systems. Journal of the American Chemical Society, 2014, 136, 17430-17433.	13.7	78
87	Synergistic geometric and electronic effects for electrochemical reduction of carbon dioxide using gold–copper bimetallic nanoparticles. Nature Communications, 2014, 5, 4948.	12.8	1,062
88	Semiconducting amorphous carbon thin films for transparent conducting electrodes. Carbon, 2014, 76, 64-70.	10.3	62
89	Superconductivity in Vacuum Annealed Bi ₆ O ₈ S ₅ . Journal of the Physical Society of Japan, 2013, 82, 034718.	1.6	22
90	Atomic distribution, local structure and cation size effect in o-R1â^'xCaxMnO3(R = Dy, Y, and Ho). Journa of Physics Condensed Matter, 2013, 25, 475901.	^{al} 1.8	6

#	Article	IF	CITATIONS
91	Atomic-scale study of topological vortex-like domain pattern in multiferroic hexagonal manganites. Applied Physics Letters, 2013, 103, 032901.	3.3	19
92	Microstructure and strain relaxation of orthorhombic TmMnO3 epitaxial thin films. Journal of Crystal Growth, 2012, 338, 280-282.	1.5	4
93	Microstructure of epitaxial YBa2Cu3O7â ^{^^} î´thin films grown on Pb(Mg1/3Nb2/3)0.7Ti0.3O3 substrates. Journal of Crystal Growth, 2012, 354, 98-100.	1.5	4
94	Microstructural Characterization of La- and Ti-Codoped Multiferroic BiFeO\$_{3}\$ Epitaxial Thin Films. IEEE Transactions on Magnetics, 2011, 47, 3780-3782.	2.1	0
95	Electric-field control of phase separation and memory effect in Pr0.6Ca0.4MnO3/Pb(Mg1/3Nb2/3)0.7Ti0.3O3 heterostructures. Applied Physics Letters, 2011, 98, .	3.3	38
96	Pitfalls in Electrochemical Liquid Cell Transmission Electron Microscopy for Dendrite Observation. Advanced Energy and Sustainability Research, 0, , 2100160.	5.8	2
97	Application of Auger electron spectroscopy in lithium-ion conducting oxide solid electrolytes. Nano Research, 0, , .	10.4	5
98	In Situ Electron Microscopy Study of the Dynamics of Liquid Flow in Confined Cells. ACS Applied Materials & Interfaces, 0, , .	8.0	1
99	Insight into ultrasensitive and high-stability flocculation-enhanced Raman spectroscopy for the <i>in situ</i>	3.5	1